

# Chapter 13

## Interaction Forest–Clearing

Thomas Foken, Andrei Serafimovich, Fabian Eder, Jörg Hübner,  
Zhongming Gao, and Heping Liu

### 13.1 Introduction

For around the last 50 years, most of the forests in the Central European hilly regions have been affected by acid rain, beetles, and windthrow. Therefore, we can no longer find any homogeneous forest sites, but rather very patchy structures with small areas of forest and clearing which are often on a scale of 1 ha or smaller. But 20–30 years ago, most of the FLUXNET sites were installed at mostly homogeneous sites. Most of the available papers are related only to the forest, and one footprint discussion

---

T. Foken (✉)  
Am Herrgottsbaum 28, 96120 Bischberg, Germany

Bayreuth Center of Ecology and Environmental Research, University of Bayreuth, Bayreuth,  
Germany  
e-mail: [foken@micrometeorology.de](mailto:foken@micrometeorology.de)

A. Serafimovich  
Helmholtz Centre Potsdam, GFZ German Research Centre for Geosciences, Telegrafenberg,  
Haus A 6, 14473 Potsdam, Germany

F. Eder  
Alexander Thamm GmbH, Wilhelm-Wagenfeld-Str. 20, 80807 München, Germany

J. Hübner  
Uhl Windkraft Projektierung GmbH & Co. KG, Max-Eyth-Str. 40, 73479 Ellwangen, Germany

Z. Gao • H. Liu  
Department of Civil & Environmental Engineering, Washington State University, 405 Spokane  
Street, Pullman, WA, 99164-2910, USA

T. Foken, A. Serafimovich, F. Eder, and J. Hübner: Affiliation during the work at the Waldstein  
sites – Department of Micrometeorology, University of Bayreuth, Bayreuth, Germany

separates forest footprints from non-forest footprints (Göckede et al. 2008). As well, clearings were the focus of researchers (Knohl et al. 2002). But the interaction between the forest and the clearing became a special research topic with the paper by Klaassen et al. (2002), who found increased fluxes at the forest edge at daytime. This study was very interesting for the discussion of the energy balance closure problem (Foken 2008), because these larger fluxes in the vicinity of the abrupt change from forest to clearing might indicate that local circulation systems are a reason for the “unclosed” energy balance. The first experimental studies were also supported by modeling projects (Sogachev et al. 2005; Klaassen and Sogatchev 2006). This was also a topic of wind tunnel studies and modeling approaches (Morse et al. 2002; Belcher et al. 2008). In these studies, it was found for the first time that the maximal flux is not at the forest edge but at a downwind distance of 5–10 canopy heights. This was underlined by several large eddy simulation (LES) studies (Dupont and Brunet 2009; Finnigan et al. 2009; Kanani-Sühring and Raasch 2015). In contrast, Schlegel et al. (2015) found from LES studies and measurements that in the case of a small-scale heterogeneous structure of the forest, the largest discontinuity of turbulence characteristics is near the forest edge.

The Waldstein–Weidenbrunnen site, together with the Köhlerloh site (see Chap. 1), is, after the Kyrill storm in 2007, an excellent natural laboratory for studying the processes highlighted above. We combine horizontal field studies presented in Chap. 14 with studies of coherent structures (Eder et al. 2013 and Chap. 6) and include all available measurements at the forest edge to give a comprehensive picture of secondary circulations, decoupling processes, and turbulent structures to support the recent discussions. The investigations were made within the EGER project and its third intensive measuring period (IOP3) from June 13 to July 26, 2011 (see Chap. 1).

## 13.2 Materials and Methods

### 13.2.1 *Special Installations at the Forest Edge*

According to the aim of the special investigation at the forest edge, a network of towers (Fig. 13.1, Table 13.1, additional to the standard installation given in Chap. 2) was installed. There was a direct line of towers from the Turbulence Tower (TT = M2) to the tower M3 at the forest edge and the tower M4 in the clearing, with turbulence measurements made at a minimum of two levels. Two additional towers (M6 and M7) were installed close to the edge, and the tower M8 was installed in the trunk space at the starting point of the horizontal moving measuring system (HMMS, Hübner et al. 2014). This system was able to measure up- and downwelling short- and longwave radiation, temperature, moisture, and CO<sub>2</sub> and O<sub>3</sub>

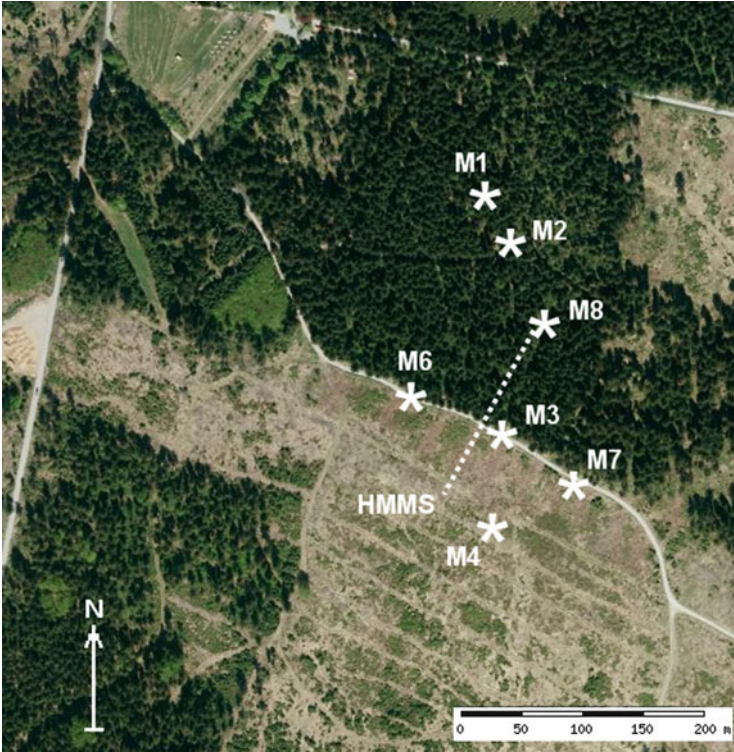


**Fig. 13.1** Waldstein–Weidenbrunnen and Köhlerloh measuring sites and positions of the Main Tower (MT = M1), the Turbulence Tower (TT = M2), the forest edge tower M3, turbulence mast M4, towers M6–M8, and horizontal mobile measuring system (HMMS). For more detail, see Serafimovich et al. (2011b). Published with kind permission of © Authors and Bayerische Vermessungsverwaltung 2011, All rights reserved

concentrations along a 150 m path at 1 m height, with half of the path in the forest and half above the clearing (see also Chap. 14). The data were corrected for the dynamical error, dependent on the response time of the applied sensors (Brock and Richardson 2001; Hübner et al. 2014). Furthermore, a CO<sub>2</sub> profile was measured at seven levels on tower M3 (0.5, 2.25, 5, 8, 13, 26, and 36 m) with a LiCor gas analyzer LI-820 and a multiplexer system. The seven heights were measured within a time period of 8 min in parallel with a temperature profile with five heights (1, 5, 18, 25, and 39 m). The system was calibrated twice a day against a CO<sub>2</sub> standard gas and zero air (nitrogen). Unfortunately, the CO<sub>2</sub> profile data are only available for the second and third Golden Day periods (July 4–8 and 14–17), and the temperature data for the first (June 26 and 28–29). For the energy balance closure investigation, net radiation measurements at M1 (top) were used for M1 and M3 (for southerly

**Table 13.1** Flux network during EGER-IOP3 (Serafimovich et al. 2011b; for tower positions, see Fig. 13.1), not all devices were used in this chapter (see also Appendix A)

Tower	Height	Sonic anemometer	Gas analyzer
M1 = MM	32 m	Metek USA-1	LiCor LI-7000
M2 = TT	36 m	Metek USA-1	LiCor LI-7500
	26 m	Metek USA-1	
	2 m	Metek USA-1	
M3	41 m	Campbell CSAT3	LiCor LI-7500
	27 m	Metek USA-1	LiCor LI-7500
	2 m	Gill HS	LiCor LI-7500
M4	5 m	Campbell CSAT3	LiCor LI-7500
	2 m	Campbell CSAT3	LiCor LI-7000
M6	5 m	Campbell CSAT3	LiCor LI-7540
	2 m	Metek USA-1	
M7	5 m	Campbell CSAT3	LiCor LI-7540
	2 m	Campbell CSAT3	
M8	2 m	Metek USA-1	

winds, the measurements at M3, 2 m height, were used). The soil heat flux in the forest was assumed to be 5 % of the net radiation. The heat storage in the biomass at noon is approximately  $5 \text{ Wm}^{-2}$ —on single days up to  $10 \text{ Wm}^{-2}$  for 2–3 h—and was included in the analysis for M1. For all other details, see Appendix A.

## 13.2.2 Methods Applied for This Investigation

### 13.2.2.1 Turbulence Data

The calculation of the turbulence data was done with the software package TK2/TK3 (Mauder and Foken 2004, 2015), which includes all relevant preprocessing and data correction tools (Foken et al. 2012b; Rebmann et al. 2012). Noteworthy are the rotation of the wind vector components by the application of a sector-wise planar fit (Wilczak et al. 2001) in order to remove the mean vertical wind within the 30-min files, the shift of the time series using the time lag of the maximum of the cross-correlation, and the application of a spike detection according to Vickers and Mahrt (1997). If the size of the data file deviated by more than 5 % from the expected file size due to data loss, the 30-min file was not processed.

For the analysis of coherent structure, the 20 Hz data were averaged to 2 Hz after collection in order to reduce computational time. This does not affect the results significantly because only high-frequency turbulence is removed. Furthermore, the time series are normalized by their mean value, and, to prevent border effects, they are extended by adding zero values at both ends. The high-frequency fluctuations

are removed by applying a low-pass filter. For this purpose, a discrete wavelet transformation with bio-orthogonal wavelets is run, which eliminates all fluctuations shorter than a critical event duration of 6.2 s (Thomas and Foken 2005).

### 13.2.2.2 Wavelet Analysis

After preparation of the 30-min files as described above, a continuous wavelet transform was performed using the Morlet wavelet, from which the wavelet power spectrum was calculated (Torrence and Compo 1998). It is possible to show the importance of different scales. For a location of individual structures in time and frequency, the Mexican Hat wavelet was used (Eder et al. 2013). If atmospheric transport is dominated by coherent structures of a certain scale, the power spectrum of the wavelet coefficients should exhibit a distinct peak at that scale. From this, it is possible to calculate the duration of coherent structures (Thomas and Foken 2005).

The first spectral peak corresponds to the coherent structures developing in the mixing layer above the forest canopy, while additional structures, e.g., which may arise from a heterogeneous canopy architecture, may cause additional peaks at larger scales in the wavelet variance spectrum (Zhang et al. 2007). In order to extract individual coherent events, the zero-crossing method serves as a detection criterion for coherent structures (Collineau and Brunet 1993a), and this proved to produce reliable results (Collineau and Brunet 1993b; Thomas and Foken 2005).

Coherent structures at high plant canopies can be divided into a sweep and an ejection. Thomas and Foken (2007a) assumed that the first half of the event is an ejection motion and the second half a sweep. Accordingly, the flux contribution of ejections ( $F_{ej}$ ) and sweeps ( $F_{sw}$ ) can be determined when the conditional averaging is applied over the relevant time intervals (Collineau and Brunet 1993a). Furthermore, Thomas and Foken (2007b) developed a method for determining the coupling of coherent structures in different levels of the canopy. For more details of this method, see Chap. 6.

For the purpose of investigation of the forest edge effect, the classification of the coupling regime after Thomas and Foken (2007b) is applied:

- Wave motion (Wa). The sub-canopy layer and forest canopy are decoupled from the layer above the canopy. Additionally, the flow above the canopy is dominated by linear gravity waves.
- Decoupled canopy (Dc). The above-canopy layer is decoupled from the canopy and the sub-canopy layers.
- Decoupled sub-canopy layer (Ds). The canopy layer is coupled to the air above the canopy, but the sub-canopy layer is still decoupled.
- Coupled sub-canopy layer by sweeps (Cs). The above-canopy and canopy layers are coupled, but the sub-canopy layer is coupled temporally only through the strong sweep motion, not through ejections.
- Fully coupled canopy (C). At all canopy levels, both ejections and sweeps contribute to the exchange of energy and matter: All canopy layers are coupled to the air above the canopy.

Because vertical and horizontal advection processes are closely connected (Aubinet et al. 2003), a similar approach for horizontal coupling was developed by Serafimovich et al. (2011a) with the coupling classes:

- Horizontal decoupled state ( $D_{c_h}$ ) with no coupling from the reference site to the observation site.
- Horizontal coupled state ( $C_h$ ). Coherent structures couple from the reference location to the observation location. The flux contribution of sweeps and ejections is larger at the observation site than at the reference site.

For more details about the data handling for the study of coherent structures, see Eder et al. (2013).

Furthermore, a continuous wavelet transformation was used to calculate local and global wavelet spectra, and an ensemble empirical mode decomposition was applied to extract dominant large-scale coherent structures (Zhang et al. 2010; Gao et al. 2016).

## 13.3 Results and Discussions

### 13.3.1 *Horizontal and Vertical Fields at the Forest Edge*

The horizontal distribution of meteorological elements measured with the HMMS was analyzed in Chap. 14. In the current chapter, only a few results from directly at the forest edge are presented. Because the largest gradients occur here, it is not easy to exactly correct the dynamical error of the response time of the sensors (Hübner et al. 2014), and the results look slightly “wavy” because the travel direction of the moving device changed from clearing–forest to forest–clearing for the next data set and so on. Figure 13.2 shows, for selected meteorological elements, a short time period in the afternoon for a sunny day. There is a very sharp change of the shortwave and longwave downwelling radiation at the forest edge. The high shortwave and the low longwave radiation measured at the clearing also influence the forest at the first few meters from the edge. Inside the forest, some sunny spots are visible. The availability of shortwave radiation is nearly unlimited in the first few meters into the forest. On the other hand, the longwave downwelling radiation is higher in the first few meters of the clearing in comparison to the data from the clearing, due to the longwave radiation of the trees. Highly interesting is the ozone distribution, which follows the distribution of the shortwave downwelling radiation in the forest but with higher ozone concentrations penetrating about 10 m further into the forest. The trunk space at a distance of about 15 m from the edge seems to be horizontally decoupled from the clearing due to low ozone concentration caused by the low radiation and possible reactions with nitrogen oxide (Foken et al. 2012a).

The most instructive vertical distribution of meteorological elements at the forest edge is the carbon dioxide concentration. Because it was measured with one

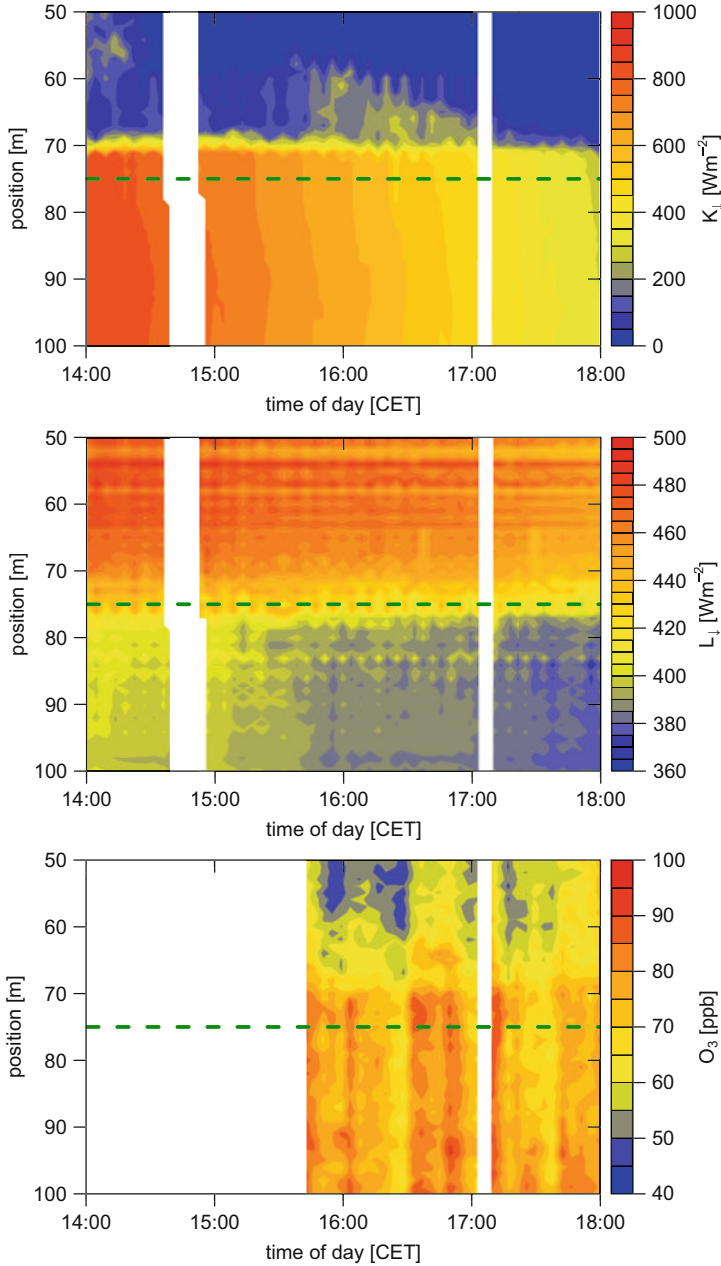


**Fig. 13.2** Detailed horizontal profiles during daytime of June 28, 2011, at the forest edge (*horizontal green dotted line*), for shortwave downwelling radiation (*above*), longwave downwelling radiation (*middle*), and ozone (*below*), corrected for dynamical errors and measured with HMMS. Position shows distance from starting point in meters, starting in the forest (50 m) and ending at the clearing (100 m) (Hübner et al. 2014, published with kind permission of © Authors 2014, CC Attribution 3.0 License, All rights reserved)

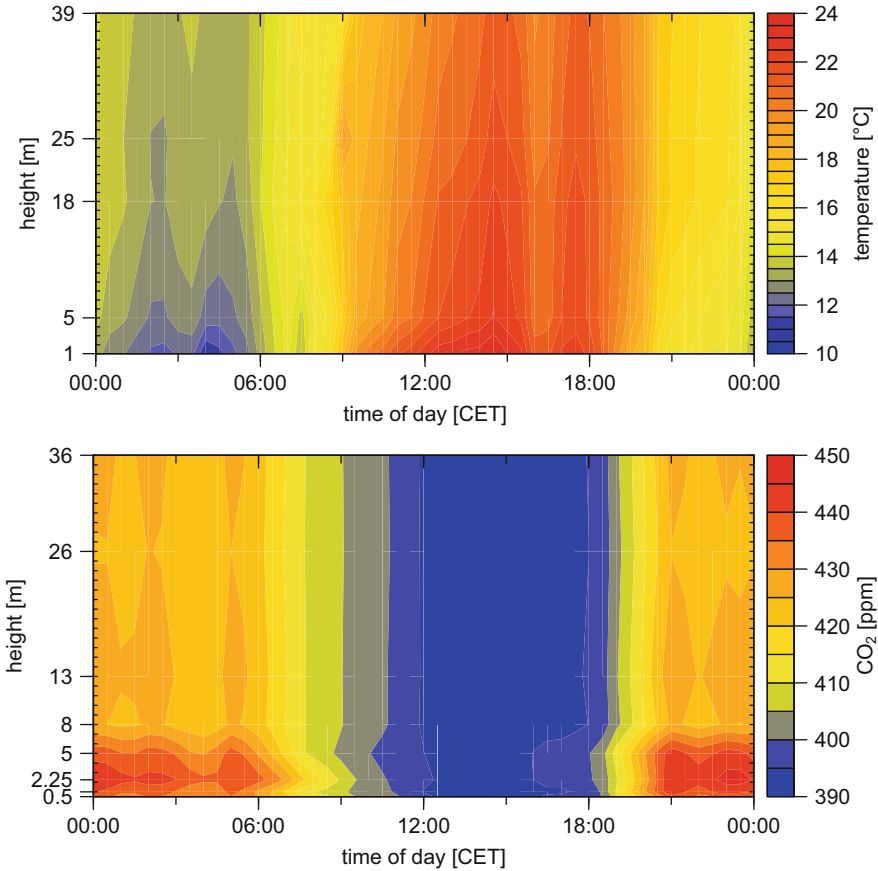


**Fig. 13.3** Profile of averaged vertical temperature (*above*) and CO<sub>2</sub> (*below*), installed at M3 at the stated heights on the axis. Half-hour averaged data are presented as a contour plot for 3 days for temperature and 7 days for carbon dioxide (Golden Days, see text) of the EGER-IOP3 period

analyzer and a multiplexer, artifacts can be excluded. Figure 13.3 shows the mean daily cycle of 7 days (second and third Golden Day period of EGER-IOP3, see Chap. 1). Noteworthy are the significantly higher carbon dioxide concentrations of a layer below 5–8 m height during the night and the morning, but already beginning at 4 p.m., which corresponds to a possible oasis effect (see Sect. 13.3.4). The parallel temperature profile shown in Fig. 13.3 (3 days of the first Golden Day period of EGER-IOP3) indicates that at the forest edge, a very stable stratification is only available in the second half on the night—in contrast to the clearing. Because the periods with a uniform daily cycle of carbon dioxide and temperature are not identical, the stability parameter  $z/L$  ( $z$ , height;  $L$ , Obukhov length) was analyzed for both periods for the clearing (M4). The strongest stable stratification is always before midnight ( $z/L \approx 0.3$ ), and the stable stratification is weaker after



midnight ( $z/L \approx 0.2$ ). Therefore, it must be assumed that the high carbon dioxide concentrations are caused by a drainage flow from the trunk space with its higher carbon dioxide concentration (see Chap. 11) and the absence of stable temperature stratification at the edge, which is only present in the second half of the night as a result of strong decoupling above the clearing. It is interesting that directly above the surface in the lowest meter, the stratification is obviously not as stable as above this layer (only visible in the carbon dioxide concentration profile with an additional measuring point at 0.5 m), which could be a result of the roughness elements in this layer.

### 13.3.2 Coupling Regime

The coupling regime was found by Foken et al. (2012a) to be an excellent indicator for the exchange process in and above the forest and for the understanding of the transport and the reaction of trace gases. The authors could also show that there is a difference in the occurrence of the coupling classes in summer and autumn. While the daily cycle of the fully coupled canopy (C) does not differ, the frequency of the decoupled situations (Wa and Dc) is much higher in autumn, even with such situations at daytime. Similar differences in the coupling regime were found between the forest (Turbulence Tower M2) and the forest edge (tower M3) according to Eder et al. (2013). The data for a summer period show a similar frequency of the fully coupled canopy (C) for both sites (Fig. 13.4). In contrast, the frequency

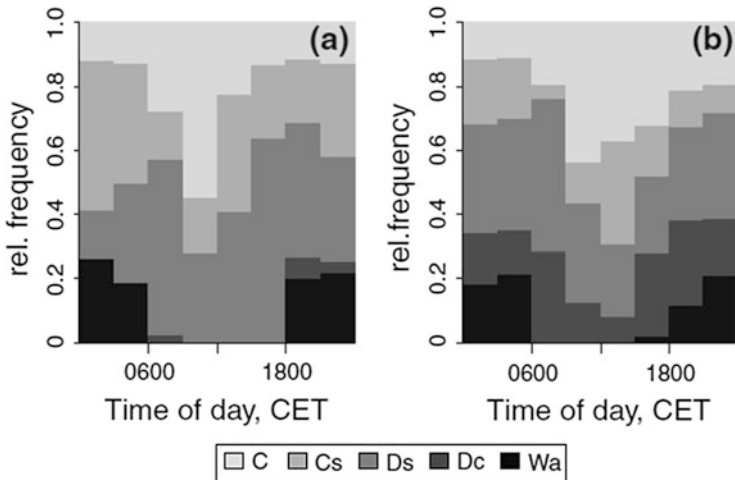


**Fig. 13.4** Relative frequency of vertical coupling regimes as a function of time of day, both within the forest at the Turbulence Tower M2 (a) and at the forest edge tower M3 (b) for the period June 21, 2011, to July 02, 2011; abbreviations of coupling regimes are according to Sect. 13.2.2 (Eder et al. 2013, published with kind permission of © Springer, Berlin, Heidelberg, All rights reserved)

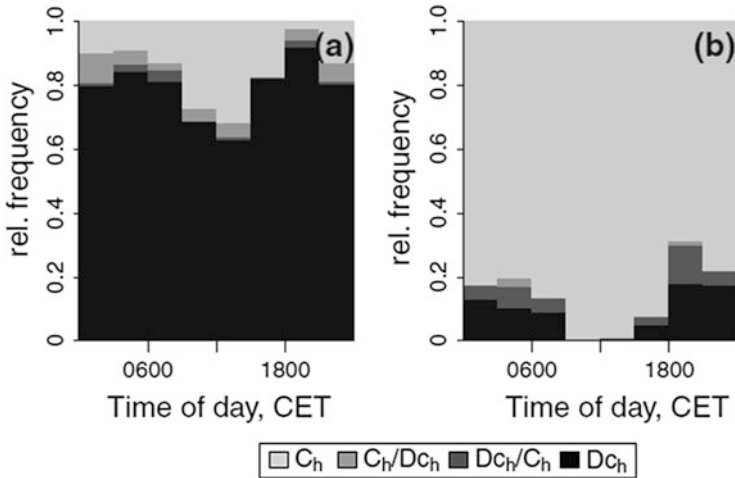


**Fig. 13.5** Relative frequency of the horizontal coupling regimes ( $C_h$ , complete coupling;  $C_h/Dc_h$ , first two towers coupled but second and third tower decoupled;  $Dc_h/C_h$ , first two towers decoupled but second and third tower coupled;  $Dc_h$ , complete decoupling) as a function of time of day, both along the transect M8–M3–M4 perpendicular to the forest edge (a) and along the transect M6–M3–M7 (b) for the measurement height at 2.25 m above ground; data from the period June 13, 2011, to July 26, 2011, were used (Eder et al. 2013, published with kind permission of © Springer, Berlin, Heidelberg, All rights reserved)

of the decoupled situations ( $Wa$  and  $Dc$ ) at the forest edge is much higher. This corresponds with the much more stable situation produced over the clearing by longwave radiation cooling, while over the forest – due to the generation of a mixing layer – mechanical turbulence is present much more often. This corresponds very well with Fig. 13.3, which shows a stable layer up to about 5 m height at the forest edge.

The frequency of the horizontal coupling perpendicular to the forest edge is comparable with the frequency of the vertically fully coupled canopy (Fig. 13.5). In all other situations, the clearing and the trunk space (75 m inside the forest at tower M8) are not coupled, and even the forest edge tower (M3) at 2.25 m height is not coupled with the clearing tower (M4). On the other hand, along the forest edge (towers M6–M3–M7), the coupling is, with the exception of some night situations, very good.

### 13.3.3 Coherent Structures

The size of coherent structures depends on the height of the canopy (Paw U et al. 1992; Finnigan 2000; Feigenwinter and Vogt 2005), and therefore, significant differences between the forest and the clearing should be found. Eder et al. (2013) investigated the event duration ( $D_e$ ) and the mean temporal separation ( $T_x$ ). In contrast, at the top of the canopy (M2 and M3) but also at the upper level (5.5 m) of the clearing tower M4, no significant differences could be found. However, the vertical profile (Fig. 13.6) shows significant differences in the trunk space at M2 and M3. The duration and the temporal separation of the structures inside the canopy are much longer than at the forest edge and above the canopy (Serafimovich et al. 2011a). Possible reasons are that only the largest structures can penetrate through the canopy (Thomas and Foken 2007b), and Dupont et al. (2012) stated that structures within the forest are linked to above-canopy coherent motions by pressure diffusion.

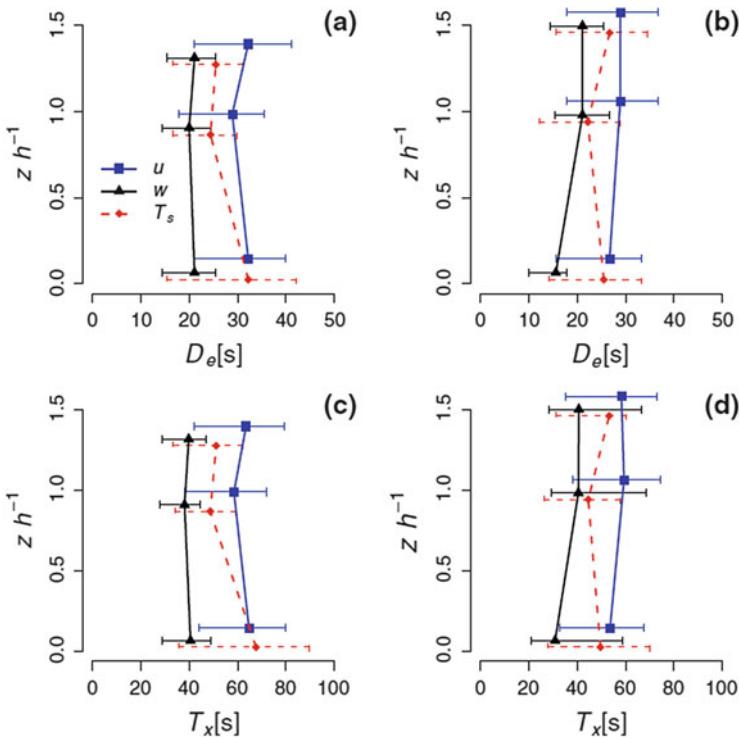


**Fig. 13.6** Vertical profiles of event durations  $D_e$  (a, b) and streamwise distances  $T_x$  (c, d) of coherent structures within the forest at the Turbulence Tower M2 (a, c) and at the forest edge tower M3 (b, d) that were detected in the time series of the horizontal wind component  $u$ , vertical wind component  $w$ , and sonic temperature  $T_s$ ; vertical axis shows measuring height  $z$  relative to canopy height  $h$ , symbols mark sample medians, and error bars represent interquartile ranges (Eder et al. 2013, published with kind permission of © Springer, Berlin, Heidelberg, All rights reserved)

Eder et al. (2013) found that the flux contribution of coherent structures is about 24–29 % above the forest for scalar fluxes and about 18 % for momentum flux. At the forest edge and the clearing, the contribution is significantly lower with 17–19 % and 12 %, respectively (Fig. 13.7a,d). This tendency is in agreement with the findings by Collineau and Brunet (1993b), who found 40 % for the sensible heat flux and 29 % for the momentum flux. The result also underlines the thesis by Dupont and Brunet (2009) that the structures need a distance of nine times the canopy height for a complete growth to occur. The highest flux contribution was found directly at the top of the canopy. In contrast, the flux contribution in the trunk space is relatively low, with 6 % for momentum flux and 15 % for buoyancy flux, which is also in agreement with literature results (Gao et al. 1989).

In the roughness sublayer above the forest, the ejection motion is stronger than at the canopy top (Fig. 13.7b,c), which is in accordance with previous studies and was reviewed in Chap. 6. When focusing on the contributions of sweeps and ejections at the forest edge (Fig. 13.7e, f), it can be stated that sweeps contribute more around the canopy top and even above the forest, but are not really significant. But at the level 2.25 m, sweeps dominate at the forest edge in contrast to the trunk space (Eder et al. 2013). It was found that in the daily cycle at the top of the towers M1 to M4, the contribution of the ejection is, for scalar and momentum fluxes, larger at daytime than at night. This effect is highly significant at the top of the forest edge tower, mainly for the momentum flux; therefore, upward convective structures at the forest edge at daytime can be postulated. The daily cycle at all towers at the lowest measuring height shows no significant differences between the towers, with more ejection at daytime than at night.

### ***13.3.4 Penetration of Large-Scale Coherent Structures***

The penetration of large coherent structures close to the surface was studied in more detail with the ensemble empirical mode decomposition (Gao et al. 2016). The analysis of single cases shows that in the wavelet structures, in the case of northerly winds and stable stratification, large coherent structures at M3 are visible only for the levels 26 and 41 m (Fig. 13.8a). In contrast, for southerly winds under stable stratification, no difference can be found in the coherent structures, including in the level 2.25 m (Fig. 13.8b). At daytime with unstable stratification, coherent structures are present at all levels and for all wavelengths, similar to Fig. 13.8b.

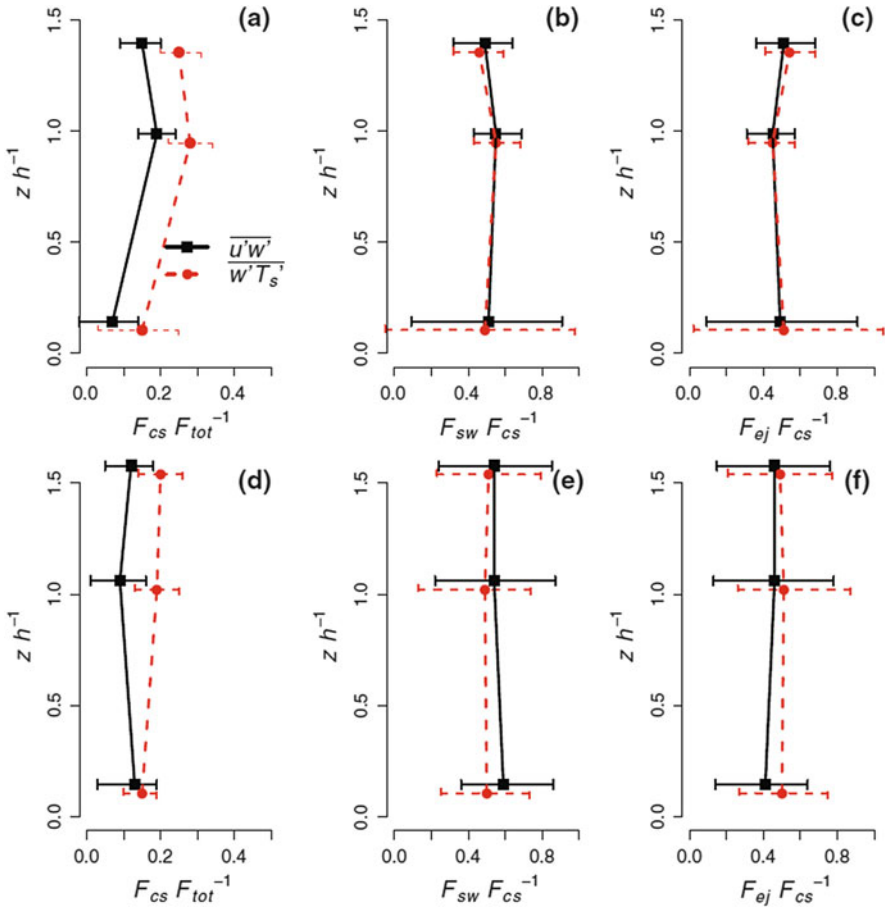


**Fig. 13.7** Vertical profiles of the relative flux contribution of coherent structures  $F_{cs} F_{tot}^{-1}$  (a, d), contributions of sweeps  $F_{sw}$  (b, e), and ejections  $F_{ej}$  (c, f) to coherent transport  $F_{cs}$  of momentum flux  $\overline{u'w'}$  and buoyancy flux  $\overline{w'T'_s}$  within the forest at M2 (a–c) and at the forest edge tower M3 (d–f); vertical axis shows measuring height  $z$  relative to canopy height  $h$ , symbols mark sample medians, and error bars represent interquartile ranges (Eder et al. 2013, published with kind permission of © Springer, Berlin, Heidelberg. All rights reserved)

This finding underlines the global spectra for the wind components (Fig. 13.9). For northerly wind, the energy is significantly lower at the 2.25 m level for all wind components. For southerly wind, the energy is nearly identical for the horizontal components. Only the vertical wind velocity has less energy – as usual – at the lower level for lower frequencies. The daytime measurements show a picture similar to the case of southerly winds.

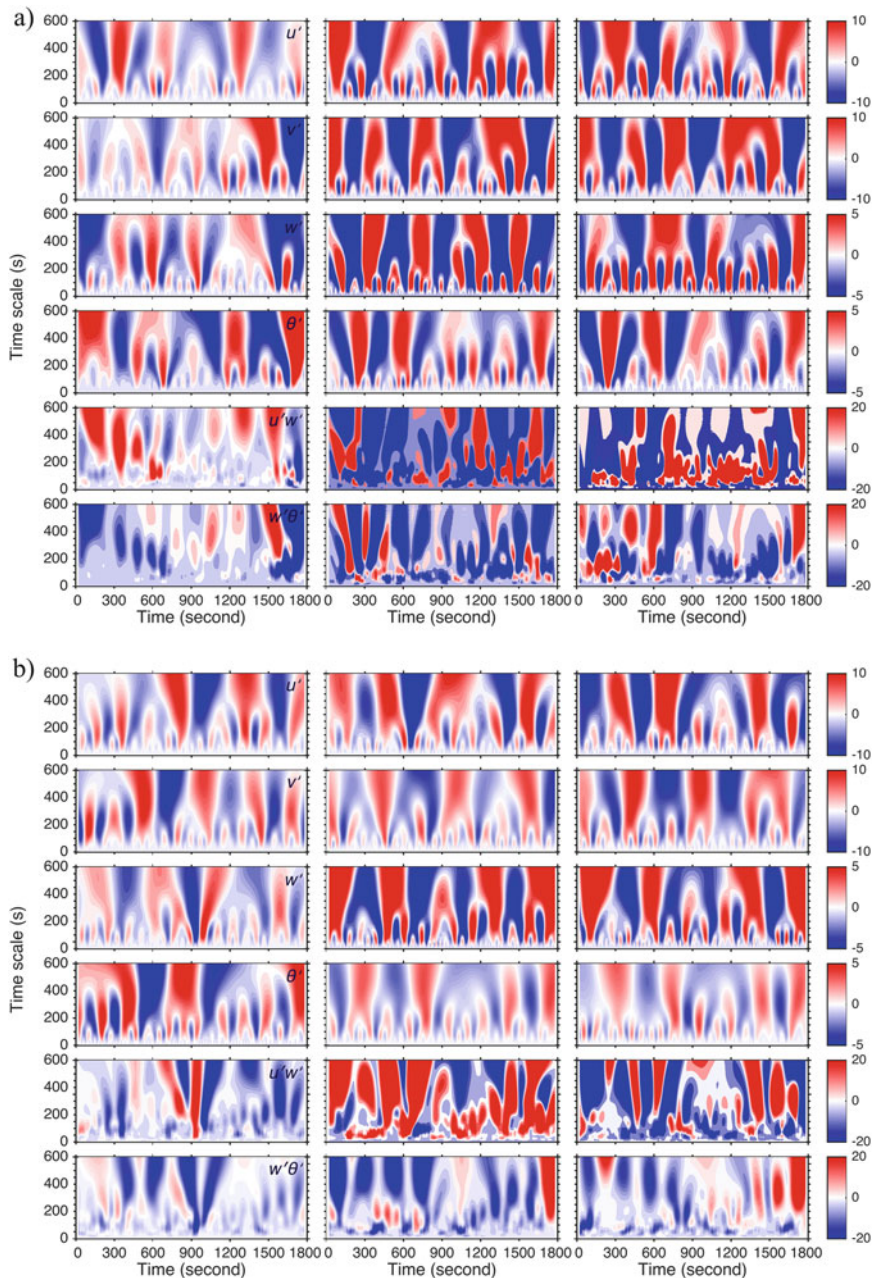


**Fig. 13.8** Local wavelet spectra for northerly winds (**a** June 23, 2011, 19:30–20:00) and southerly winds (**b** June 22, 2011, 05:30–06:00). In the columns are shown from left to right the levels 2.25, 26, and 41 m, and in the lines from top to bottom the horizontal wind components along the mean wind direction and perpendicular to the mean wind direction, the vertical wind component, the temperature, the momentum flux, and the buoyancy flux

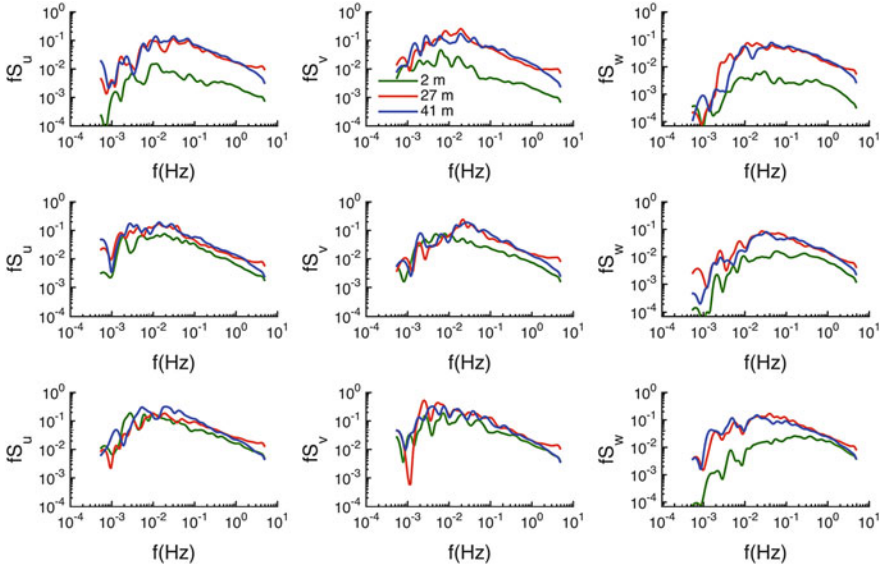


**Fig. 13.9** Global wavelet spectra at three levels of tower M3 for the horizontal wind components in the mean wind direction ( $u$ , left side), perpendicular to the mean wind direction ( $v$ , middle), and for the vertical wind component ( $w$ , right side) with the frequency  $f$ . The upper panel shows the situation for stable stratification and northerly winds (June 23, 2011, 19:30–20:00, at 2.25 m:  $0.32 \text{ ms}^{-1}$ ,  $16^\circ$ ), the middle panel for stable stratification and southerly wind (June 22, 2011, 05:30–06:00, at 2.25 m:  $0.88 \text{ ms}^{-1}$ ,  $175^\circ$ ), and the lower panel for unstable stratification at daytime (June 21, 2011, 14:30–15:00, at 2.25 m:  $1.4 \text{ ms}^{-1}$ ,  $272^\circ$ )

### 13.3.5 Energy Balance Closure Problem

Of special interest was the direct determination of the energy balance closure (Fig. 13.10), which was corrected for the heat storage in the canopy. The Bowen ratio is typically  $Bo > 1$  for a spruce forest in summer. In contrast, at the forest edge (only cases with wind direction from the clearing were analyzed) and on the clearing, the Bowen ratio is  $Bo < 1$ , and it is lower in the late afternoon than during the day. This is an indicator for a small oasis effect. The net radiation at the Main Tower (M1) was also used for the forest edge tower M3 and was higher than in the clearing (M4). The residual at M1 was significantly higher, with up to about  $200 \text{ Wm}^{-2}$  at noon in comparison to both of the other towers with  $100\text{--}150 \text{ Wm}^{-2}$ . In approximate terms, in the afternoon from 3 p.m., the residual is nearly zero. This is an indicator of higher turbulent fluxes at the forest edge. More details about energy balance closure can be found in Chaps. 4 and 12.

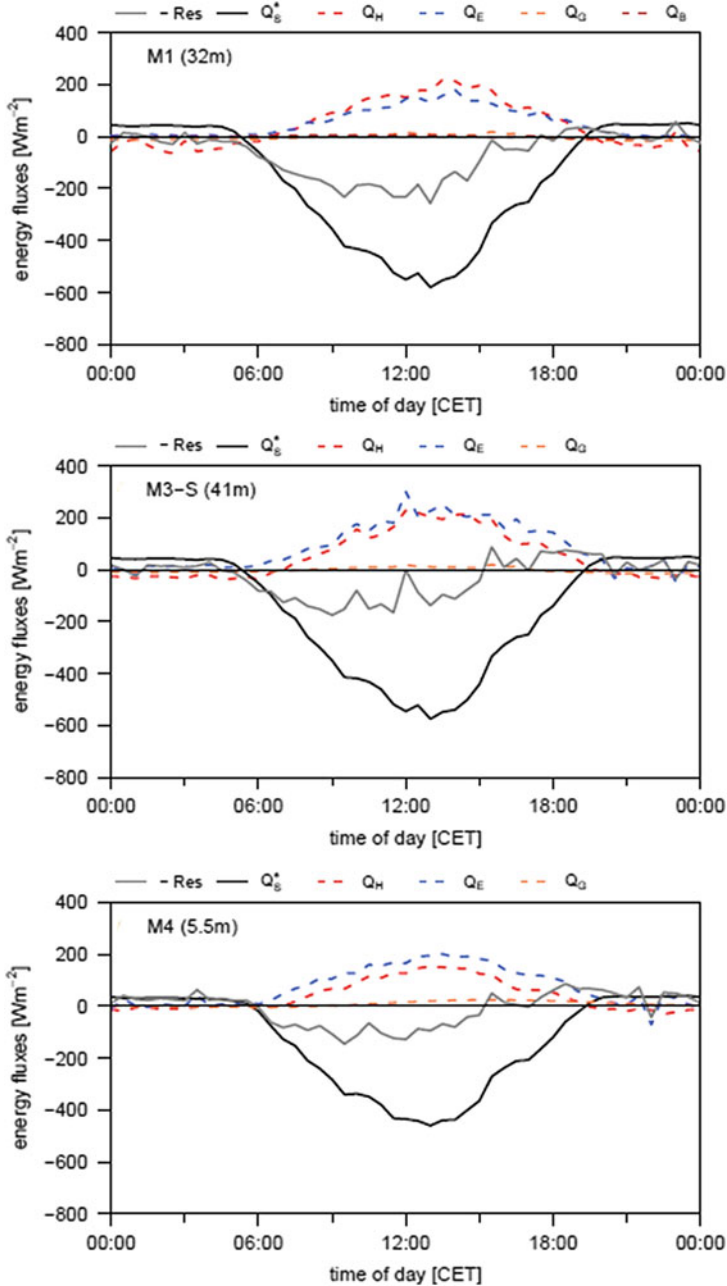


**Fig. 13.10** Mean diurnal cycles of the observed energy fluxes along the transect perpendicular to the forest edge for 13 days (Golden Days) of the EGER-IOP3 period. Measurements were performed above the forest at M1 (*above*), at the forest edge at 41 m (M3, *middle*), and at the clearing (M4, *below*), with  $Q_H$ , sensible heat flux;  $Q_E$ , latent heat flux;  $Q_G$ , ground heat flux;  $Q_s^*$ , net radiation;  $Res$ , residual of the energy balance closure



## 13.4 Conclusions

The puzzle of the presented results invites an interesting discussion about the conditions at the forest edge: The conclusions are not final statements but form a request for further discussion or even research. For final conclusions, see Chap. 19.

Of surprise is the apparent low horizontal coupling. This may be a real effect according to the shown horizontal distribution of ozone but could also reflect a problem with the methodology. Because the horizontal structures are much longer in the forest sub-canopy than at the forest edge, but the analyzing methods look only for the first (shortest) significant structure (Thomas and Foken 2007a; Serafimovich et al. 2011a), it may be possible that the longer structures are also present at the clearing but that shorter structures are dominant. At daytime, the length of the first coherent structure is, due to the better vertical coupling, nearly identical at both sites, and therefore, the method indicates a horizontal coupling. This thesis can be underlined by the good horizontal coupling of the three towers along the forest edge, even under very stable stratification.

The strength of the horizontal coupling could also explain differences in the LES, with a flow maximum at a certain distance from the edge (Dupont and Brunet 2009; Finnigan et al. 2009; Kanani-Sühring and Raasch 2015) and no such maximum in other investigations (Schlegel et al. 2015). In nature, the sub-canopy vegetation is very dense at the forest edge, which can be responsible for the decoupling. If the LES model has a homogeneous tree structure up to the edge, the penetration of air can be large in the trunk space at the forest edge and can be a reason for the strong updrafts at a certain distance from the edge. This should be tested in further LES studies with a reduced airflow into the forest at the edge.

The different horizontal and vertical decoupling may also be affecting the interpretation of advection. The hypothesis of a closed mass balance by horizontal and vertical advection (Aubinet et al. 2003) is not realistic – even when the slope is about 3°, as at the Waldstein–Weidenbrunnen site – under such coupling situations. The alternative hypothesis that the horizontal CO<sub>2</sub> concentration differences are caused by the varying degree to which coherent structures affect the sub-canopy air exchange (see Chap. 6) may be more realistic. However, the two hypotheses may in fact be complementary: Spatially varying penetration depths of turbulent coherent structures may give rise to gradients that lead to horizontal advection by mean flow. Whether the two hypotheses are compatible mainly depends on the time scale at which coherent structures, horizontal concentration differences, and thus gradients occur. Near the forest edge, a drainage flow of carbon dioxide-rich air already starting at the late afternoon (oasis effect) was detected.

The lower turbulent fluxes and the large residual of the energy balance closure above the forest (M1) can also be interpreted in two ways: If the findings by LES (Dupont and Brunet 2009; Finnigan et al. 2009; Kanani-Sühring and Raasch 2015) that a maximal flux is at a distance from the forest edge of about ten times of the canopy height are true, then at the position of M1 (about five times the canopy height), the flux should be lower and not representative for the forest as a whole. On

the other hand, the larger turbulent fluxes at the forest edge in comparison to M1 and the clearing can also fulfill the energy balance closure concept (Foken 2008), with its large fluxes at heterogeneities, and it is in agreement with experimental findings by Klaassen et al. (2002).

Interesting is the decoupling at the forest edge occurring mainly in the second half of the night, while at the clearing (Fig. 13.10 for M4), the strongest stable stratification is—as usual—in the first half of the night. At the forest edge, the stabilization of the stratification due to longwave cooling is probably compensated by a warm drainage flow from the forest and a better vertical coupling. The large-scale coherent structures do not penetrate into this drainage flow (Figs. 13.8 and 13.9 for northerly winds). This may be a topic of further research, because the experimental design used was not adapted to investigate such processes. But such research could have a very practical aim, because the specific emissions of the variously sized clearings found in the increasingly heterogeneous forests are unknown and the few available studies cannot answer this question (Knohl et al. 2002).

No clear conclusion can be drawn about the existence of a secondary circulation. Eder et al. (2013) already concluded that the strong ejections at the forest edge can be an indication of a secondary circulation. In addition, the larger residual above the forest in comparison to the forest edge is a second criterion. Furthermore, the Köhlerloh clearing is large enough to generate convective processes (Shen and Leclerc 1997) and has unstable conditions with low wind speeds (Eigenmann et al. 2009). However, such situations are difficult to see with the sodar, although one situation was found by Foken et al. (2012a). Unfortunately, Doppler lidar measurements were not funded for this experiment. Such an experiment—combination of lidar measurements and LES modeling—was realized above the larger but isolated Yatir forest in Israel. Eder et al. (2015), using measurements and LES modeling, found secondary circulations which had a contribution to the turbulent fluxes of 19 %, slightly smaller than the typical closure gap at the Waldstein–Weidenbrunnen site (Chap. 12), with 17 % at the forest edge and about 25 % above the forest and the clearing. Therefore, it is not presumptuous to postulate the existence of secondary circulations for the Waldstein–Weidenbrunnen site as well, at least at daytime. Whether the size of the heterogeneities is related to forest–clearing or to forest areas–agricultural areas in the surroundings is still a question of further research (see also Chaps. 12 and 19).

**Acknowledgment** This research was funded by the German Science Foundation within the DFG PAK 446 project, mainly the subproject FO226/21-1. H. Liu acknowledges support by the National Science Foundation AGS under grant 1419614. The heat storage in the biomass was calculated by Kathrin Gatzsche in her master's thesis.

## References

- Aubinet M, Heinesch B, Yernaux M (2003) Horizontal and vertical CO<sub>2</sub> advection in a sloping forest. *Bound-Lay Meteorol* 108:397–417
- Belcher SE, Finnigan JJ, Harman IN (2008) Flows through forest canopies in complex terrain. *Ecol Appl* 18:1436–1453
- Brock FV, Richardson SJ (2001) *Meteorological measurement systems*. Oxford University Press, New York, 290 pp
- Collineau S, Brunet Y (1993a) Detection of turbulent coherent motions in a forest canopy. Part I: Wavelet analysis. *Bound-Lay Meteorol* 65:357–379
- Collineau S, Brunet Y (1993b) Detection of turbulent coherent motions in a forest canopy. Part II: Time-scales and conditional averages. *Bound-Lay Meteorol* 66:49–73
- Dupont S, Brunet Y (2009) Coherent structures in canopy edge flow: a large-eddy simulation study. *J Fluid Mech* 630:93–128
- Dupont S, Irvine M, Bonnefond J-M, Lamaud E, Brunet Y (2012) Turbulent structures in a pine forest with a deep and sparse trunk space: stand and edge regions. *Bound-Lay Meteorol* 143:309–336
- Eder F, Serafimovich A, Foken T (2013) Coherent structures at a forest edge: properties, coupling and impact of secondary circulations. *Bound-Lay Meteorol* 148:285–308
- Eder F, De Roo F, Rotenberg E, Yakir D, Schmid HP, Mauder M (2015) Secondary circulations at a solitary forest surrounded by semi-arid shrubland and their impact on eddy-covariance measurements. *Agric For Meteorol* 211–212:115–127
- Eigenmann R, Metzger S, Foken T (2009) Generation of free convection due to changes of the local circulation system. *Atmos Chem Phys* 9:8587–8600
- Feigenwinter C, Vogt R (2005) Detection and analysis of coherent structures in urban turbulence. *Theor Appl Climatol* 81:219–230
- Finnigan J (2000) Turbulence in plant canopies. *Annu Rev Fluid Mech* 32:519–571
- Finnigan JJ, Shaw RH, Patton EG (2009) Turbulence structure above a vegetation canopy. *J Fluid Mech* 637:687–424
- Foken T (2008) The energy balance closure problem – an overview. *Ecolog Appl* 18:1351–1367
- Foken T, Meixner FX, Falge E, Zetzsch C, Serafimovich A, Bargsten A, Behrendt T, Biermann T, Breuninger C, Dix S, Gerken T, Hunner M, Lehmann-Pape L, Hens K, Jocher G, Kesselmeier J, Lüers J, Mayer JC, Moravek A, Plake D, Riederer M, Rütz F, Scheibe M, Siebicke L, Sörgel M, Staudt K, Trebs I, Tsokankunku A, Welling M, Wolff V, Zhu Z (2012a) Coupling processes and exchange of energy and reactive and non-reactive trace gases at a forest site – results of the EGER experiment. *Atmos Chem Phys* 12:1923–1950
- Foken T, Leuning R, Oncley SP, Mauder M, Aubinet M (2012b) Corrections and data quality. In: Aubinet M et al (eds) *Eddy covariance: a practical guide to measurement and data analysis*. Springer, Dordrecht, pp 85–131
- Gao W, Shaw RH, Paw U KT (1989) Observation of organized structure in turbulent flow within and above a forest canopy. *Bound-Lay Meteorol* 47:349–377
- Gao Z, Liu H, Russell ES, Huang J, Foken T, Oncley SP (2016) Large eddies modulating flux convergence and divergence in a disturbed unstable atmospheric surface layer. *J Geophys Res: Atmos* 121:1475–1492
- Göckede M, Foken T, Aubinet M, Aurela M, Banza J, Bernhofer C, Bonnefond J-M, Brunet Y, Carrara A, Clement R, Dellwik E, Elbers JA, Eugster W, Fuhrer J, Granier A, Grünwald T, Heinesch B, Janssens IA, Knohl A, Koeble R, Laurila T, Longdoz B, Manca G, Marek M, Markkanen T, Mateus J, Matteucci G, Mauder M, Migliavacca M, Minerbi S, Moncrieff JB, Montagnani L, Moors E, Ourcival J-M, Papale D, Pereira J, Pilegaard K, Pita G, Rambal S, Rebmann C, Rodrigues A, Rotenberg E, Sanz MJ, Sedlak P, Seufert G, Siebicke L, Soussana JF, Valentini R, Vesala T, Verbeeck H, Yakir D (2008) Quality control of CarboEurope flux data – part I: Coupling footprint analyses with flux data quality assessment to evaluate sites in forest ecosystems. *Biogeosci* 5:433–450

- Hübner J, Olesch J, Falke H, Meixner FX, Foken T (2014) A horizontal mobile measuring system for atmospheric quantities. *Atmos Meas Tech* 7:2967–2980
- Kanani-Sühring F, Raasch S (2015) Spatial variability of scalar concentrations and fluxes downstream of a clearing-to-forest transition: A Large-Eddy Simulation study. *Bound-Lay Meteorol* 155:1–27
- Klaassen W, Sogatchev A (2006) Flux footprint simulation downwind of a forest edge. *Bound-Lay Meteorol* 121:459–473
- Klaassen W, van Breugel PB, Moors EJ, Nieveen JP (2002) Increased heat fluxes near a forest edge. *Theor Appl Climatol* 72:231–243
- Knohl A, Kolle O, Minayeva TY, Milyukova IM, Vygodskaya NN, Foken T, Schulze ED (2002) Carbon dioxide exchange of a Russian boreal forest after disturbance by wind throw. *Glob Chang Biol* 8:1–16
- Mauder M and Foken T (2004) Documentation and instruction manual of the eddy covariance software package TK2. *Arbeitsergeb, Univ Bayreuth, Abt Mikrometeorol* 26:42 pp. ISSN 1614-8916
- Mauder M and Foken T (2015) Documentation and Instruction Manual of the Eddy-Covariance Software Package TK3 (update). *Arbeitsergeb, Univ Bayreuth, Abt Mikrometeorol* 62:64. ISSN 1614-8916
- Morse AP, Gardiner BA, Marshall BJ (2002) Mechanisms controlling turbulence development across a forest edge. *Bound-Lay Meteorol* 103:227–251
- Paw U KT, Brunet Y, Collineau S, Shaw RH, Maitani T, Qiu J, Hipps L (1992) On coherent structures in turbulence above and within agricultural plant canopies. *Agric For Meteorol* 61:55–68
- Rebmann C, Kolle O, Heinesch B, Queck R, Ibrom A, Aubinet M (2012) Data acquisition and flux calculations. In: Aubinet M et al (eds) *Eddy covariance: a practical guide to measurement and data analysis*. Springer, Dordrecht, pp 59–83
- Schlegel F, Stiller J, Bienert A, Maas H-G, Queck R, Bernhofer C (2015) Large-eddy simulation study of the effects on flow of a heterogeneous forest at sub-tree resolution. *Bound-Lay Meteorol* 154:27–56
- Serafimovich A, Thomas C, Foken T (2011a) Vertical and horizontal transport of energy and matter by coherent motions in a tall spruce canopy. *Bound-Lay Meteorol* 140:429–451
- Serafimovich A, Eder F, Hübner J, Falge E, Voß L, Sörgel M, Held A, Liu Q, Eigenmann R, Huber K, Duarte HF, Werle P, Gast E, Cieslik S, Liu H and Foken T (2011b) ExchanGE processes in mountainous regions (EGER)- documentation of the intensive observation period (IOP3) June, 13th to July, 26th 2011. *Arbeitsergeb, Univ Bayreuth, Abt Mikrometeorol* 47:135. ISSN 1614-8916
- Shen S, Leclerc MY (1997) Modelling the turbulence structure in the canopy layer. *Agric For Meteorol* 87:3–25
- Sogachev A, Leclerc MJ, Karipot A, Zhang G, Vesala T (2005) Effect of clearcuts on footprints and flux measurements above a forest canopy. *Agric For Meteorol* 133:182–196
- Thomas C, Foken T (2005) Detection of long-term coherent exchange over spruce forest. *Theor Appl Climatol* 80:91–104
- Thomas C, Foken T (2007a) Organised motion in a tall spruce canopy: temporal scales, structure spacing and terrain effects. *Bound-Lay Meteorol* 122:123–147
- Thomas C, Foken T (2007b) Flux contribution of coherent structures and its implications for the exchange of energy and matter in a tall spruce canopy. *Bound-Lay Meteorol* 123:317–337
- Torrence C, Compo GP (1998) A practical guide to wavelet analysis. *Bull Am Meteorol Soc* 79:61–78
- Vickers D, Mahrt L (1997) Quality control and flux sampling problems for tower and aircraft data. *J Atmos Oceanic Tech* 14:512–526

- Wilczak JM, Oncley SP, Stage SA (2001) Sonic anemometer tilt correction algorithms. *Bound-Lay Meteorol* 99:127–150
- Zhang G, Thomas C, Leclerc MY, Karipot A, Gholz HL, Foken T (2007) On the effect of clearcuts on turbulence structure above a forest canopy. *Theor Appl Climatol* 88:133–137
- Zhang Y, Liu H, Foken T, Williams QL, Liu S, Mauder M, Liebethal C (2010) Turbulence spectra and cospectra under the influence of large eddies in the energy balance experiment (EBEX). *Bound-Lay Meteorol* 136:235–251